BRAIN
CLINICAL TRIAL

Venglustat combined with imiglucerase for neurological disease in adults with Gaucher disease type 3: the LEAP trial

Raphael Schiffmann,[1,†] Timothy M. Cox,[2] Jean-François Dedieu,[3] Sebastiaan J. M. Gaemers,[4] Julia B. Hennermann,[5] Hiroyuki Ida,[6] Eugen Mengel,[5,7] Pascal Minini,[8] Pramod Mistry,[9] Petra B. Musholt,[10] David Scott,[11] Jyoti Sharma[12] and M. Judith Peterschmitt[13]

Gaucher disease type 3 is a chronic neuronopathic disorder with wide-ranging effects, including hepatosplenomegaly, anaemia, thrombocytopenia, skeletal disease and diverse neurological manifestations. Biallelic mutations in *GBA1* reduce lysosomal acid β-glucosidase activity, and its substrates, glucosylceramide and glucosylsphingosine, accumulate. Enzyme replacement therapy and substrate reduction therapy ameliorate systemic features of Gaucher disease, but no therapies are approved for neurological manifestations. Venglustat is an investigational, brain-penetrant, glucosylceramide synthase inhibitor with potential to improve the disease by rebalancing influx of glucosylceramide with impaired lysosomal recycling. The Phase 2, open-label LEAP trial (NCT02843035) evaluated orally administered venglustat 15 mg once-daily in combination with maintenance dose of imiglucerase enzyme replacement therapy during 1 year of treatment in 11 adults with Gaucher disease type 3. Primary endpoints were venglustat safety and tolerability and change in concentration of glucosylceramide and glucosylsphingosine in CSF from baseline to Weeks 26 and 52. Secondary endpoints included change in plasma concentrations of glucosylceramide and glucosylsphingosine, venglustat pharmacokinetics in plasma and CSF, neurologic function, infiltrative lung disease and systemic disease parameters. Exploratory endpoints included changes in brain volume assessed with volumetric MRI using tensor-based morphometry, and resting functional MRI analysis of regional brain activity and connectivity between resting state networks. Mean (SD) plasma venglustat $AUC_{0\text{-}24}$ on Day 1 was 851 (282) ng•h/ml; C_{max} of 58.1 (26.4) ng/ml was achieved at a median t_{max} 2.00 h. After once-daily venglustat, plasma concentrations (4 h post-dose) were higher compared with Day 1, indicating ~2-fold accumulation. One participant (Patient 9) had low-to-undetectable venglustat exposure at Weeks 26 and 52. Based on mean plasma and CSF venglustat concentrations (excluding Patient 9), steady state appeared to be reached on or before Week 4. Mean (SD) venglustat concentration at Week 52 was 114 (65.8) ng/ml in plasma and 6.14 (3.44) ng/ml in CSF. After 1 year of treatment, median (inter-quartile range) glucosylceramide decreased 78% (72, 84) in plasma and 81% (77, 83) in CSF; median (inter-quartile range) glucosylsphingosine decreased 56% (41, 60) in plasma and 70% (46, 76) in CSF. Ataxia improved slightly in nine patients: mean (SD, range) total modified Scale for Assessment and Rating of Ataxia score decreased from 2.68 [1.54 (0.0 to 5.5)] at baseline to 1.55 [1.88 (0.0 to 5.0)] at Week 52 [mean change: −1.14 (95% CI: −2.06 to −0.21)]. Whole brain volume increased slightly in patients with venglustat exposure and biomarker reduction in CSF (306.7 ± 4253.3 mm^3) and declined markedly in Patient 9 (−13894.8 mm^3). Functional MRI indicated stronger connectivity at Weeks 26 and 52 relative to baseline between a broadly distributed set of brain regions in patients with venglustat exposure and biomarker reduction but not Patient 9, although neurocognition, assessed by Vineland II, deteriorated in all domains over time, which illustrates disease progression despite the intervention. There were no deaths, serious adverse events or discontinuations. In adults with Gaucher disease type 3 receiving imiglucerase, addition of once-daily venglustat showed acceptable safety and tolerability and preliminary evidence of clinical stability with intriguing but intrinsically inconsistent signals in selected biomarkers, which need to be validated and confirmed in future research.

Received February 16, 2022. Revised August 15, 2022. Accepted September 11, 2022.. Advance access publication October 18, 2022

1 Institute of Metabolic Disease, Baylor Scott and White Research Institute, Dallas, TX 75246, USA
2 Department of Medicine, University of Cambridge and Addenbrooke's Hospital, Cambridge CB2 0QQ, UK
3 Neurology Development, Sanofi, 91385 Chilly-Mazarin, France
4 Global Pharmacovigilance, Sanofi, Amsterdam, 1105 BP, The Netherlands
5 Center for Pediatric and Adolescent Medicine Villa Metabolica, University Medical Center Mainz, 55131 Mainz, Germany
6 Department of Pediatrics, The Jikei University School of Medicine, Tokyo 105-8461, Japan
7 Clinical Science for LSD, SphinCS, 65239 Hochheim, Germany
8 Biostatistics and Programming, Sanofi, 91385 Chilly-Mazarin, France
9 Yale Lysosomal Disease Center and Gaucher Disease Treatment Center, Yale School of Medicine, New Haven, CT 06510, USA
10 R&D Global Development, Sanofi, 65926 Frankfurt, Germany
11 Medical and Scientific Affairs, Neuroscience, Clario, San Mateo, CA 94404, USA
12 Pharmacokinetics, Dynamics and Metabolism, Sanofi, Bridgewater, NJ 08807, USA
13 Neurology Clinical Development, R&D, Sanofi, Cambridge, MA 02141, USA
† Present address: Texas Neurology, Dallas, TX 75246, USA

Correspondence to: Raphael Schiffmann, MD, MHSc, FAAN
Texas Neurology
6080 N Central Expy, Ste 100, Dallas, TX 75246, USA
E-mail: rschiffmann@texasneurology.com

Keywords: Gaucher disease type 3; venglustat; substrate reduction therapy; glycosphingolipids; CNS

Introduction

Gaucher disease (GD) is a rare, lysosomal storage disorder caused by biallelic mutations in the *GBA1* gene, thereby reducing acid β-glucosidase activity with consequent accumulation of its primary substrate, glucosylceramide (GL-1 or Gb1) (Fig. 1), mainly in the lysosomal compartment of macrophages and, in the neuronopathic variants, also in neurons.[1] Cellular accumulation of glucosylceramide and related sphingolipids causes multisystem disease with diverse clinical features, including hepatosplenomegaly, anaemia, thrombocytopenia, skeletal disease, variable neurological manifestations, lung involvement and growth failure in children.[1]

GD is operationally classified into three phenotypes. Type 1 (GD1) is characterized by absence of CNS involvement until adult life when Parkinson disease and/or dementia may develop in a minority of patients. The haematological, visceral and skeletal manifestations are successfully treated with intravenous enzyme replacement therapy or oral substrate reduction therapy. Type 2 (GD2) and type 3 (GD3) are the neuronopathic forms. GD2 is characterized by infantile onset of rapidly progressive neurodegenerative disease, which is fatal in the first years of life. In GD3, CNS involvement is typically apparent months to years after birth, and neurological progression is slower than in GD2; many patients survive into adulthood.[2] Individuals with GD3 have the non-neurological features of GD1 and diverse neurological manifestations, including horizontal supranuclear gaze palsy (considered a defining feature of the disease subtype). There is variable cognitive impairment, particularly affecting executive functions, that develops in childhood and tends to spare speech and language; motor and coordination deficits such as ataxia; hyperreflexia without a pyramidal syndrome; tremor (mostly cerebellar or action tremor); partial complex or generalized seizures; stridor; dysphagia; dysarthria; dysmetria; dystonia; behavioural abnormalities and progressive myoclonic epilepsy.[2–5] In most patients with GD3 who had undergone splenectomy, accumulation of glucosylceramide and glucosylsphingosine was observed in the cerebrum and cerebellum.[6] In the few autopsies of patients with GD3, there was little or variable neuronal loss, suggesting that while existing neurons may be affected, they retain the potential for recovery.[7–10]

Currently, there are no approved therapies for the neurological manifestations of GD3. Enzyme replacement therapy, which effectively ameliorates non-neurological manifestations,[11] does not cross the blood–brain barrier and studies in GD3 patients showed no evidence of cognitive or oculomotor improvement.[12–15] Eliglustat, a glucosylceramide synthase inhibitor approved as first-line therapy in GD1 patients, is also excluded from the brain.[16] Miglustat, a substrate reduction therapy with weak inhibitory activity on glucosylceramide synthase, is partially distributed to the brain but is ineffective for neurological symptoms.[17] Miglustat is approved as second-line therapy for patients with non-neurological GD, for whom enzyme replacement therapy is not a therapeutic option.[18]

Venglustat (formerly known as GZ/SAR402671) is an investigational, orally administered, brain-penetrant glucosylceramide synthase inhibitor with potential to treat neuronopathic manifestations of GD3. Venglustat is a novel, potent and specific inhibitor of glucosylceramide formation (Fig. 1).[19] Another glucosylceramide synthase inhibitor, eliglustat, is approved as first-line therapy for treatment of the non-neuronopathic features of GD but is not able to achieve distribution in the brain. In mouse models of neurological GD, venglustat has decreased glycosphingolipid synthesis and reduced accumulation of gluco-series glycolipids in the liver and brain, extent of gliosis and severity of ataxia and paresis. Median survival increased from 45 to 60 days (30%) for treated mice[19] (expected lifespan for wild-type mice is 2 years). In a Phase 1, multiple ascending dose study of venglustat in healthy volunteers, once-daily venglustat dosing of up to 15 mg resulted in a time- and dose-dependent decrease of plasma glucosylceramide and a favourable safety and tolerability profile.[20] Modelling of pharmacokinetic-pharmacodynamic relations after repeated dosing indicated an E_{max} of 80% for venglustat, which was closely approached

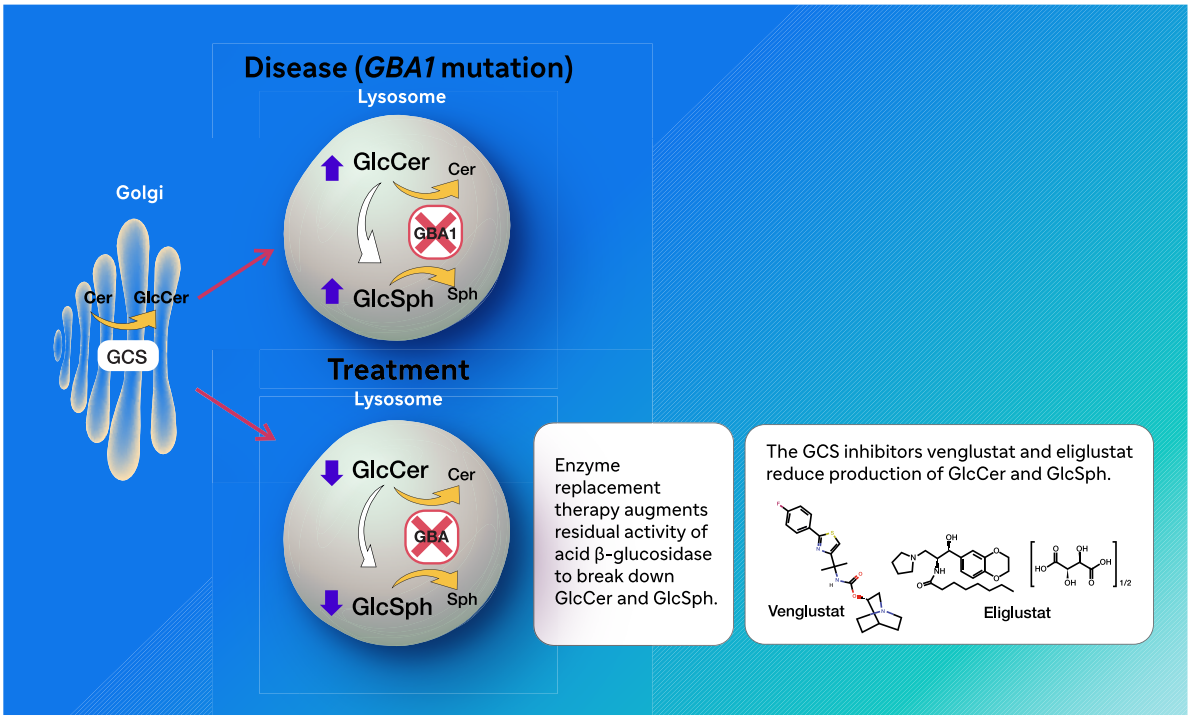

Figure 1 Glycosphingolipid biosynthesis in GD and mechanisms by which treatments correct the underlying metabolic defect. *Top*: Glucosylceramide (GlcCer) and gluco-series sphingolipids are generated from ceramide and glucose by UDP-glucosylceramide synthase (UCGC) in the cis-Golgi. The reaction is common to the *de novo* and salvage pathways for glycosphingolipid biosynthesis from glucose (Glc) and ceramide (Cer). GD arises because of impaired activity of the lysosomal enzyme, acid β-glucosidase. As a result, its substrates, GlcCer and glucosylsphingosine (GlcSph), accumulate in the lysosome and in cell membranes and bring about GD. *Bottom*: Enzyme replacement therapy with recombinant human acid β-glucosidase restores enzymatic function and with it, the recycling of glycosphingolipids. However, enzyme therapy is not readily delivered to the brain. Brain-penetrant inhibitors of glucosylceramide biosynthesis, such as venglustat, attenuate formation of β-glucosylceramide and β-glucosylsphingosine in the brain and allow the lysosome to rebalance synthesis of glycosphingolipids with the rate of recycling—thereby alleviating the toxic build-up of glucosylceramides and their metabolites. Note: after biosynthesis in the Golgi, GlcCer is distributed throughout the cell and dynamically recycled by lysosomes in the constitutive process of membrane fusion.

following administration of 15 mg venglustat, with mean plasma glucosylceramide reduction of 74.6% from baseline on Day 15.[20] This dose and dosing regimen was selected for investigation in venglustat trials in GD3 patients.

Here we report the 1-year safety and efficacy outcomes from the first trial of venglustat in patients with GD3 with chronic neuronopathic manifestations whose systemic disease had been stabilized by enzyme replacement therapy.

Materials and methods

Study design

The Phase 2 open-label LEAP trial (NCT02843035) evaluated treatment with oral venglustat (Sanofi, Cambridge, MA, USA) in combination with intravenous imiglucerase (Cerezyme, Sanofi, Cambridge, MA, USA) in adults with GD3 at six academic medical centres in the USA, Europe and Japan. Patients ingested venglustat 15 mg once daily in addition to their maintenance dose of imiglucerase administered intravenously every 2 weeks (maintenance dose was tailored by the investigator-assessed response of each patient's systemic disease manifestations to enzyme therapy). The primary outcome was assessed after 1 year of treatment (52 weeks) and the long-term extension phase (208 weeks) is ongoing. The study was conducted in accordance with the Declaration of Helsinki and International Conference on Harmonisation guidelines for good clinical practice. The study protocol was approved by the institutional review board or ethics committee at each participating site. Informed consent was obtained from all patients before participation in the study.

Eligible patients

Adults aged ≥18 years with a clinical diagnosis of GD3, documented deficiency of acid β-glucosidase activity in peripheral blood leukocytes, and gaze palsy were eligible, provided they had received imiglucerase therapy for ≥3 years and at a stable dose for ≥6 months before enrolment. Patients were also required to meet the following pre-defined GD therapeutic goals: haemoglobin concentration ≥11.0 g/dl (women) or ≥12.0 g/dl (men), platelet count $\geq 100 \times 10^9$/l, spleen volume <10 multiples of normal, liver volume <1.5 multiples of normal and to be free of symptomatic bone disease over the preceding year. The patients were required to have either an intact spleen or to have undergone total splenectomy >3 years before enrolment. Venglustat is principally metabolized by the CYP3A cytochrome complex; therefore, avoidance of grapefruit, grapefruit juice or grapefruit containing products was required. Patients with a history of seizures (other than myoclonic seizures) were eligible provided seizures were well controlled with medication that was neither a strong nor a moderate inducer or inhibitor of CYP3A. Patients were recruited through regular clinical visits, physician outreach to existing patients, physician referrals and advertisement at patient advocacy groups and medical congress.

Study end points

The primary endpoints were safety and tolerability of venglustat in combination with imiglucerase and change in concentration of the direct GD biomarkers glucosylceramide and glucosylsphingosine (lyso-GL-1 or lyso-Gb1) in CSF from baseline to Weeks 26 and 52. For assessment of GD biomarkers, CSF was collected by lumbar puncture at baseline and Weeks 1, 4, 26 and 52 and plasma and serum were collected at baseline and Weeks 1, 4, 12, 26, 39 and 52. Secondary endpoints included change in plasma concentrations of glucosylceramide and glucosylsphingosine, venglustat pharmacokinetics in plasma and CSF, horizontal and vertical saccades, ataxia and neurocognitive function. A complete listing of assessments performed in the LEAP study is provided in Supplementary Table 1.

Plasma samples for pharmacokinetic analysis were collected pre-dose and 1, 2, 4, 8 and 24 h after dosing on Day 1; at 2 to 4 h after dosing at Weeks 4, 26 and 52 and pre-dose at Weeks 12 and 39. CSF samples for pharmacokinetics were collected pre-dose on Day 1 and 2 to 4 h after dosing at Weeks 4, 26 and 52. The following plasma pharmacokinetic parameters were calculated using a noncompartmental method after dosing on Day 1: maximum plasma concentration (C_{max}); time to C_{max} (t_{max}); area under the plasma concentration versus time curve from 0 to 24 h ($AUC_{0–24}$). In addition, trough plasma venglustat concentration observed immediately before venglustat dosing (C_{trough}) and 4-h post-dose plasma venglustat concentrations measured at pre-defined visits were summarized with descriptive statistics. Pharmacokinetics in the CSF were examined 4 h after dosing, and venglustat concentrations were measured at pre-defined visits and summarized by descriptive statistics.

A pathognomonic feature of neuronopathic GD is the presence of gaze palsy, which typically affects horizontal saccade initiation.[2] Quantification of horizontal and vertical saccadic eye movements was recorded using a non-invasive technique and assessed by a central reader (Eye See Tec). Eye position and target data were filtered to obtain eye velocity. Saccades were detected using velocity criteria and their amplitude, duration and peak velocity were determined.

Ataxia was assessed with the Scale for Assessment and Rating of Ataxia (SARA), an eight-item clinical scale (gait, stance, sitting, speech, finger-chase test, nose-finger test, fast alternating movements and heel-shin test) based on semiquantitative assessment of cerebellar ataxia on impairment level.[21] SARA yields a total score from 0 (no ataxia) to 40 (very severe ataxia). The US Food and Drug Administration requested use of the total modified SARA score, which is a simplified scoring system that adjusts scoring particularly for the gait, stance and speech disturbance domains. In the total modified SARA score, each item is scored on a 0 to 4 scale, resulting in a total scale of 0–32.

The Trail Making Test (TMT) was used to evaluate neurocognitive function. This test assesses visual search, scanning, speed of processing, mental flexibility and executive functions.[22] Part A (TMT-A) assesses a combination of visual search and general visual and motor processing speed: it mainly evaluates perceptual and psychomotor speed. Part B (TMT-B) assesses mental flexibility and shifting abilities and, since the individual must actively switch between categories, is considered to include an executive function component.[23] The TMT-B minus TMT-A score was used to remove the variance attributable to the graphomotor and visual scanning components of TMT-A.[22] This derived score reflects the unique task requirements of TMT-B. Adaptive function was evaluated using the Vineland Adaptive Behavior Scale II.[24]

The following exploratory biomarkers were quantified in CSF: ceramide, the precursor and a metabolite of glucosylceramide; chitotriosidase, an enzyme indicative of macrophage activation that is known to be elevated in GD[25]; and monosialodihexosylganglioside, a glycosphingolipid related to glucosylceramide also known to be elevated in GD.[26] Glycoprotein non-metastatic melanoma protein B, which has been reported as a biomarker of pathological macrophages in GD3,[27] was quantified in CSF.

The following non-neuronopathic systemic manifestations of GD were assessed according to standard clinical practice: haemoglobin concentration, platelet count, liver and spleen volumes, bone marrow burden score, bone mineral density, bone pain and bone crisis.[28,29] Dual energy X-ray absorptiometry was performed to evaluate bone mineral density. MRI scans of the lumbar spine and femur were used to evaluate bone marrow infiltration using the bone marrow burden score.[30] Pulmonary function testing (standardized in accordance with American Thoracic Society guidelines[31]) included spirometry to assess forced vital capacity (FVC), forced expiratory volume in the first second of the FVC manoeuvre (FEV_1), and total lung capacity. Diffusing capacity of carbon monoxide was used to measure gas exchange across the alveolocapillary membrane.

EEG was carried out at baseline, Week 26 and Week 52 with patients at rest in the supine position in a quiet, dimly lit room; the leads were recorded for ~30 minutes. Provocation methods with hyperpnoea and intermitted light stimulation were performed systematically for all EEGs.

Brain imaging

Exploratory endpoints included changes in brain volume assessed with volumetric MRI (vMRI) using tensor-based morphometry, and resting functional MRI (fMRI) analysis of regional brain activity and connectivity between resting state networks (RSNs). MRI of the brain and brainstem, with minimum T1 and T2 sequences, was done at baseline, Week 26 and Week 52 on 1.5 and 3 T magnets manufactured by GE, Philips and Siemens. MRI data were processed, read and analysed centrally by an independent reviewer blinded to patient identity and time point (Clario).

MRI of the brain and brain stem was used to evaluate anatomical structures and to assess volume (vMRI) using FreeSurfer version 5.3 (FreeSurfer project, The General Hospital Corporation, Boston, MA, USA) anatomic parcellation and tensor-based morphometry analysis cycle. Assessment of atrophy using tensor-based morphometry (also known as Jacobian Integration) consists of estimating the volume changes as captured within the deformation fields resulting from applying a symmetric deformable registration technique between a pair of MRI scans (baseline and follow-up), using a non-linear symmetric log-demons deformation technique with a robust cross-correlation metric to ensure invertibility of the transformation (symmetric process).[32] The deformation field is then analysed by computing the determinant of its Jacobian matrix, which is a measure of local volume change. An integration of the determinant over a brain region of interest provides an estimate of the rate of change in volume of this region over time.

Resting fMRI analysis was conducted to assess the effects of treatment on regional brain activity using the blood-oxygenation level dependent response. fMRI preprocessing was carried out according to established practices.[33–36] Anatomical regions of interest

were defined using masks generated by the complete FreeSurfer segmentation. Parcellation of the baseline high-resolution 3D-T1 structural image was performed to derive connectivity between the complete set of FreeSurfer-derived anatomical regions. Full and partial connectivity were computed between the RSNs 1, 2, 3, 6, 7 and 8 using the template maps developed by Smith *et al*.[37]

RSNs are anatomically distinct but functionally connected brain regions with strongly correlated blood flow signal (i.e. with synchronous fluctuations in brain activity). The medial occipital (RSN 1), occipital pole (RSN 2) and lateral occipital (RSN 3) areas are linked to visual perception, as well as to broader cognitive domains including spatial pattern recognition and language comprehension. RSN 6 corresponds strongly with motor tasks, encompassing supplementary, primary and secondary motor cortices, and is linked with both action and perception behavioural paradigms.[37,38] RSN 7 is assigned to the 'auditory' domain, although its constituent regions, including superior temporal and posterior insular cortex, also map onto action-execution-speech, cognition-language-speech and perception domains. RSN 8 includes subregions within medial frontal and anterior cingulate cortex, underlying 'executive control' and cognitive domains, such as action-inhibition, emotion and perception-somesthesia-pain.

Statistical analyses

Clinical, laboratory and MRI endpoints were analysed in a descriptive manner at scheduled visits. There was no pre-specified statistical testing; sample size and trial duration were primarily determined by feasibility rather than formal sample size calculation.

Data availability

Data underlying the findings described in this article may be obtained in accordance with the Sanofi data sharing policy described at https://www.sanofi.com/en/science-and-innovation/clinical-trials-and-results/our-data-sharing-commitments.

Results

Patients

Between March 2017 and December 2018, 16 patients with GD3 were screened, of which 11 patients enrolled and were treated with the combination of venglustat and imiglucerase. All 11 patients completed the 52-week treatment phase. There were seven men and four women (six white, three Asian, two African American) with a mean age at enrolment of 25 years (range: 18–32). Molecular analysis of *GBA1* revealed the following genotypes: eight patients were p.Leu483Pro homozygotes [p.Leu483Pro/p.Leu483Pro (L444P/L444P)], two were compound heterozygotes for p.Leu483Pro [p.Phe252Ile/p.Leu483Pro (F213I/L444P)] and one was a compound heterozygote for the pathological p.Asp448His and p.Arg502Cys alleles (D409H/R463C). The stable dose of imiglucerase ranged from 38.5 to 125 U/kg body weight biweekly.

Venglustat pharmacokinetics

After the first dose, the mean (SD) plasma venglustat $AUC_{0\text{-}24}$ on Day 1 was 851 (282) ng•h/ml and mean (SD) plasma C_{max} of 58.1 (26.4) ng/ml was achieved at a median t_{max} of 2.00 h.

Venglustat concentrations in plasma and CSF are shown for individual patients in Fig. 2. One patient (Patient 9) had 50% lower plasma and CSF venglustat concentrations at Week 26 (53.3 and 1.77 ng/ml, respectively) compared with Week 4 (102 and 3.05 ng/ml respectively) and undetectable (i.e. below the lower limit of quantification [LLOQ]) venglustat concentrations at Week 52. This patient was therefore excluded from descriptive statistics of PK parameters. Mean (SD) plasma venglustat concentrations in the remaining 10 patients (measured ~4 h post-dose) were 48 (17.5), 116 (48.1), 120 (40.1) and 114 (65.8) ng/ml at Day 1 and Weeks 4, 26 and 52, respectively, indicating ~2-fold accumulation and that steady state was reached on or before Week 4. Mean (SD) CSF venglustat concentrations were 6.63 (2.42), 6.77 (1.96) and 6.14 (3.44) ng/ml at Weeks 4, 26 and 52, respectively, indicating that steady state was reached on or before Week 4. The higher variability in plasma and CSF concentrations at Week 52 may be attributed to the lower venglustat concentrations observed in another study participant (Patient 1) compared with Week 26, which we attribute to temporary co-administration of venglustat with the CYP3A inducer, rifampin, during Weeks 42 to 55. Since venglustat is a CYP3A substrate, concomitant administration with CYP3A inducers is predicted to reduce systemic exposure to venglustat.

Direct and indirect biomarkers of GD

Over 1 year of venglustat treatment, concentrations of glucosylceramide and glucosylsphingosine in plasma and CSF decreased markedly in 10 out of 11 patients; Patient 9, in whom venglustat exposure was low-to-undetectable at Weeks 26 and 52, did not achieve sustained reduction in these disease-related metabolites (Fig. 3). Among all 11 patients from baseline to Week 52, median (inter-quartile range) glucosylceramide decreased from 5.23 μg/ml (4.78, 7.00) to 1.10 μg/ml (0.92, 1.86) in plasma and 5.70 μg/ml (4.53, 8.02) to 1.00 (1.00 2.15) in CSF, and glucosylsphingosine decreased from 19.30 ng/ml (8.78, 48.90) to 14.80 ng/ml (2.50, 18.40) in plasma and from 43.20 pg/ml (21.3, 56.0) to 11.50 pg/ml (5.8, 28.0) in CSF. These improvements represent median (95% CI) glucosylceramide reductions of 78% (46 to 84) in plasma and 81% (47 to 83) in CSF and glucosylsphingosine reductions of 56% (23 to 60) in plasma and 70% (45 to 76) in CSF. In *post hoc* analysis, venglustat concentration in CSF at Week 4 was inversely correlated with glucosylceramide concentration in plasma ($r = -0.719$, $P = 0.013$) and in CSF ($r = -0.536$, $P = 0.110$) (Supplementary Fig.1).

Concentrations of exploratory biomarkers in CSF over 1 year of venglustat treatment are shown in Supplementary Fig. 2. Ceramide concentrations in CSF were within reference ranges at baseline and throughout the study. Glycoprotein non-metastatic melanoma protein B concentrations in CSF were not elevated at baseline. Two patients were homozygous for duplicated *CHIT1* alleles and had no detectable plasma chitotriosidase activity. Among the eight patients who had detectable chitotriosidase activity and sustained exposure to venglustat (i.e. Patient 9 excluded), mean (SD) chitotriosidase activity in CSF decreased 29% (18.5) at Week 52. The pathological ganglioside, monosialodihexosylganglioside, was measurable in CSF at baseline in eight of 11 patients but was undetectable in all CSF samples taken at Weeks 4, 26 and 52.

Saccades

After 1 year of venglustat treatment, there was no clear evidence of a treatment effect on saccadic eye movements (horizontal or vertical velocity and amplitude measurements).

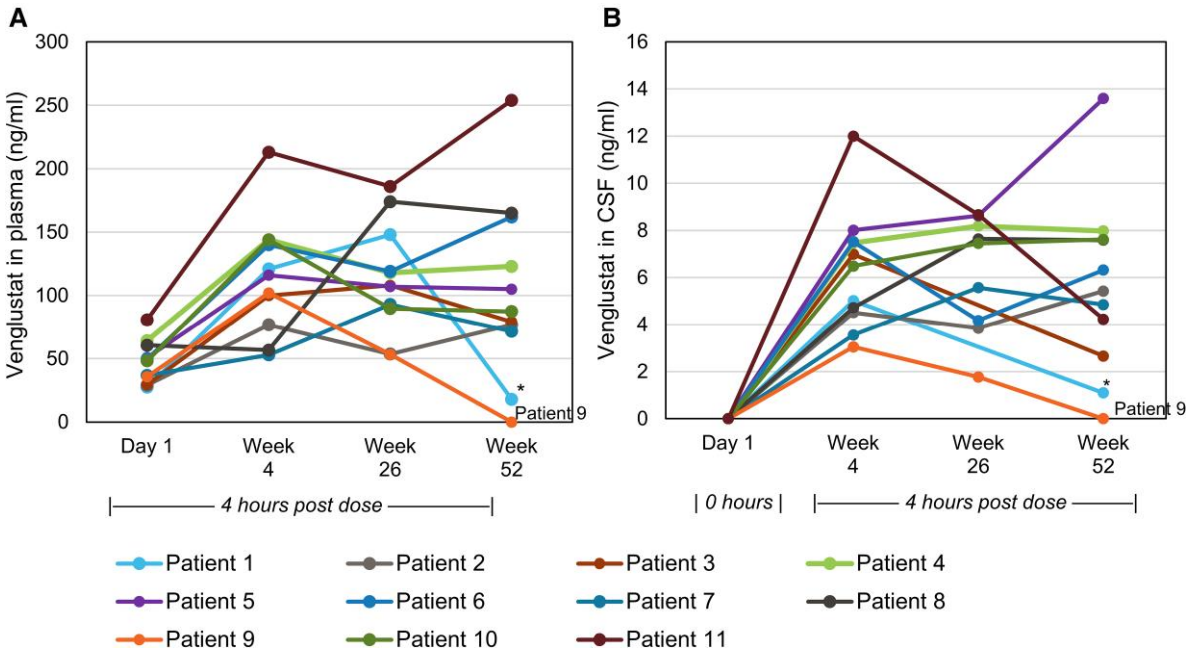

Figure 2 Individual venglustat concentrations in plasma (A) and CSF (B). Concentrations measured ~4 h post-dose. *Denotes values < LLOQ entered as 0.

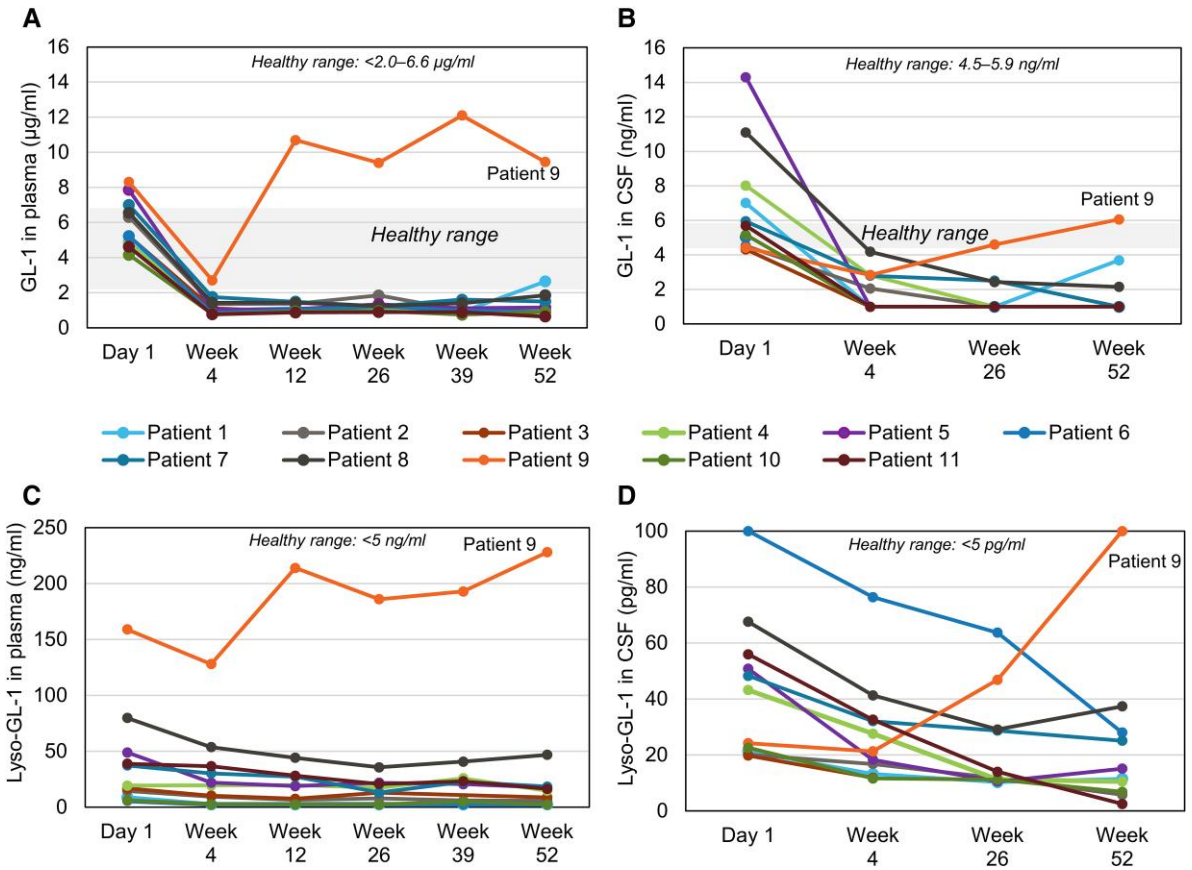

Figure 3 Plasma and CSF concentrations of glucosylceramide (A and B) and glucosylsphingosine (C and D) from baseline to Week 52. LLOQ: plasma glucosylceramide 0.1 µg/ml, CSF glucosylceramide 2.0 ng/ml, plasma glucosylsphingosine 5.0 ng/ml, CSF glucosylsphingosine 5 pg/ml.

Ataxia

Ten of 11 patients demonstrated mild ataxia (total SARA score ≥0.5) at baseline. The most common deficits noted at baseline were gait and stance disorders; seven patients had impaired gait and/or stance at baseline as reflected by scores of 1 or 2 on SARA items 1 and 2. No patients had difficulty sitting (SARA item 3) during the study. The one patient with mild speech disturbance (SARA item 4) at baseline improved during the study.

Original and modified total SARA scores had identical mean [SD (range)] values of 2.68 [1.54 (0.0 to 5.5)] at baseline and 1.55 [1.88 (0.0 to 5.0)] at Week 52, respectively. Total modified SARA score improved slightly in nine of 11 patients (one patient's score was stable at 0 for all time points, one patient's score worsened) (Fig. 4A), with a mean change from baseline of −1.14 points (95% CI: −2.06 to −0.21). For this analysis, the 'stance' score (SARA item 2) at Week 52 for Patient 8 was replaced with the score from Week 26, due to an injury (knee pain and left great toe injury) at the Week 52 assessment that precluded objective assessment. The patient with low venglustat exposure (Patient 9) had a baseline total modified SARA score of 0.5 and subsequently improved to a score of 0 at Week 52. This improvement may reflect variability of SARA scoring after repeated assessments.

Neurocognition

From baseline to Week 52, mean (SD) time to complete TMT Trail A remained stable from 54.4 (47.5) s at baseline to 53.5 (43.1) s at Week 52 [mean change: −0.8 (95% CI: −21.0 to 19.4)]; 5 of 11 patients exhibited a minor reduction. Time to complete TMT Trail B decreased from 153.6 (149.4) to 115.3 (76.8) seconds [mean change: −38.4 (95% CI: −104.8 to 28.1)]; 8 of 11 patients exhibited a marked reduction. TMT scores for Trail B result minus Trail A result remained stable or improved in all patients (Fig. 4B). The mean [SD (range)] difference in time to complete Trail B minus time to complete Trail A decreased from 99.3 s [107.5 (13 to 410)] at baseline to 61.7 s [46.2 (6 to 166)] at Week 52 [mean change: −37.5 (95% CI: −88.1 to 13.0)]; 7 of 11 patients exhibited a reduction. The time to complete Trail B minus time to complete Trail A was markedly longer than normative values in subjects without any history of neurological or psychiatric symptoms, where the mean (SD) Trail B result minus Trail A result was 30.55 (16.14) s in subjects <20 years of age ($n = 10$) and 44.61 (27.75) in subjects 20–29 years of age ($n = 66$).[39]

On the baseline Vineland II assessment, the mean (SD) Adaptive Behavior composite score [7.8 (20.9)], Communication domain score [71.7 (21.2)] and Daily Living Skills domain score [80.3 (21.0)] were moderately low, and the mean (SD) for Socialization domain score [85.6 (20.7)] was adequate. All domains decreased in normative score over 1 year of venglustat treatment, indicating that this population was behind peers in these areas of functioning at baseline and the disease deteriorated despite the pharmacological intervention.

Brain volumetric MRI

Eight of 11 patients had analysable vMRI images for all three study time points and sustained exposure to venglustat (hereafter, vMRI Group A). The vMRI for Patient 9 was available and, owing to low venglustat exposure, is reported separately; vMRI data was not analysable for Patient 2 and Patient 11 since they had metal dental implants that compromised the imaging. The tensor-based morphometry cycle showed that mean whole brain volume increased slightly in vMRI Group A (306.7 ± 4253.3 mm^3 from a baseline volume of 1 220 800 ± 139 508 mm^3) after 1 year of venglustat treatment; in contrast, whole brain volume decreased markedly (−13894.8 mm^3 from a baseline volume of 882 951 mm^3) in Patient 9 who had low venglustat exposure. Within-subject change from baseline in whole brain volume showed slight increases in five vMRI Group A patients, slight decreases in three vMRI Group A patients, and a more marked decrease in Patient 9 (Table 1). Fig. 5 shows the nine brain regions with the greatest increases in volume for vMRI Group A patients compared with decreases in eight of these nine regions in Patient 9 (mean atrophy ± SD: right accumbens area 12.9 ± 9.6, left putamen 94.7 ± 78.7, left entorhinal 34.5 ± 32.1, right putamen 97.8 ± 100.8, right postcentral 91.7 ± 100.0, left pericalcarine 18.5 ± 22.0, right amygdala 60.8 ± 74.9, left cuneus 37.2 ± 46.2, left lingual 50.1 ± 80.0, ventricle volume −438 ± 696.9). As a reciprocal corollary to regional brain volume, the mean volume of the cerebral ventricles decreased in vMRI Group A, while in Patient 9, ventricular volume increased, reflecting a progressive loss of brain tissue amounting to nearly 14 ml.

Brain functional MRI

Nine of 11 patients had analysable fMRI images for all three study time points and sustained venglustat exposure (hereafter, fMRI Group A). The fMRI for Patient 9 was available and, because of the low venglustat exposure, is reported separately. Owing to the metal implant, the fMRI for Patient 2 could not be analysed, however, after the use of field-map correction, fMRI for Patient 11 (also with a dental implant) could be analysed.

Patients in fMRI Group A demonstrated stronger connectivity at Weeks 26 and 52 relative to baseline between a broadly distributed set of brain regions, with enhanced occipito-parietal connectivity as the most prominent feature. At the functional level, evidence of enhanced connectivity in fMRI Group A patients was strongest between functional RSNs 1, 2 and 3 ('perception-vision', 'cognition-language-orthography' and 'cognition-space', respectively) and RSNs 6, 7 and 8 ('sensorimotor', 'auditory' and 'executive control', respectively) (Fig. 6). The increases in connectivity strength yielded strong effect sizes (Cohen's $d > 0.8$), with a maximal increased correlation coefficient of 0.19 ± 0.16. Increased connectivity between these RSNs reflects greater functional correspondence between posterior, parietal and frontal brain areas, and suggests enhanced integration of bottom-up and top-down cognitive processes. At the anatomical level, fMRI Group A patients showed a widespread and robust strengthening of connections between occipital-parietal structures and frontal, temporal and limbic targets. On the other hand, in Patient 9, these longitudinal effects were much less consistent and often in the negative direction; connectivity changes were more modest and restricted to spatially proximal structures (Fig. 6).

EEG

EEG results without stimulation, with hyperpnea stimulation and with light stimulation were normal at baseline in nine of 11 patients, including five patients with normal EEG results at all time points. One patient had abnormal EEG with and without stimulation at baseline, Week 26 and Week 52, and one had abnormal EEG only without stimulation at baseline and Week 52. Four patients had occasional abnormal EEG results: three patients at Week 26 and one patient at Week 52.

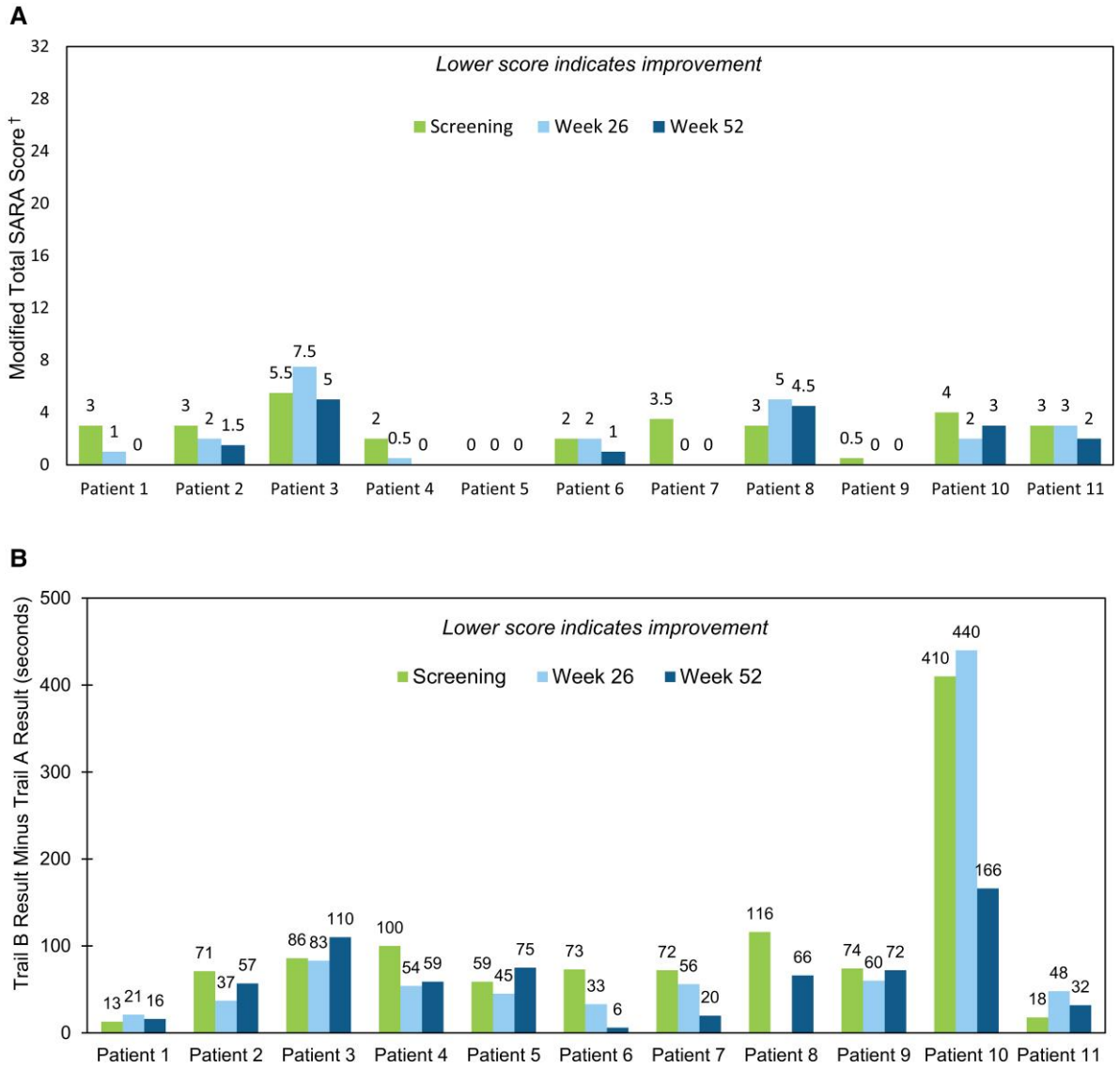

Figure 4 Total modified SARA score (A) and TMT-B minus TMT-A score (B) at screening, Weeks 26 and 52. In the total modified SARA score, each item of the SARA scale is scored on a 0 to 4 scale (possible range 0–32) and higher scores indicate more severe ataxia. Normative values for time to complete Trail B minus time to complete Trail A in subjects without any history of neurological or psychiatric symptoms: mean (SD) 30.55 (16.14) s in subjects <20 years of age ($n = 10$) and 44.61 (27.75) s in subjects 20–29 years of age ($n = 66$).[39]

Systemic manifestations

As study participants had been on imiglucerase therapy for ≥3 years, their haematological, organ volume, skeletal and lung parameters of GD were predicted to remain stable and did so in nearly all cases (Supplementary Fig. 3). Haemoglobin concentrations, platelet counts and spleen and liver volumes were within the reference range for healthy persons at baseline and remained in this range throughout 1 year of venglustat treatment. Among the seven patients with lumbar spine bone mineral density data, five patients remained in the same bone density category after 1 year of venglustat treatment and two patients changed categories (one from normal to osteopaenia and one from osteopaenia to osteoporosis). Bone marrow burden scores during 1 year of treatment remained in the same severity category in 10 patients and worsened from mild to moderate in one patient. Two patients experienced bone pain, none experienced a bone crisis or fracture and one patient developed an osteolytic lesion. Among the seven patients who had detectable interstitial lung disease at baseline, four improved after 1 year of venglustat treatment. The patient with low venglustat exposure (Patient 9) showed deterioration of interstitial lung disease from baseline to 1 year. Among the four patients without baseline opacity on lung imaging, none had new opacities after 1 year of venglustat treatment. Eight patients showed no or mild impairments on baseline pulmonary function tests, including spirometry. Two patients exhibited moderate deterioration from baseline to 1 year on DL_{CO}, TLC and/or FEV_1 or FVC assessment.

Safety

After 1 year of venglustat exposure in combination with imiglucerase, no deaths or serious adverse events were reported and no patient discontinued the study treatment. All 11 patients experienced at least one adverse event. Adverse events reported in two or more

Table 1 Changes in individual patient parameters from baseline to Week 52

Patient no.	Venglustat concentration in CSF at Week 52 (ng/ml)	Glucosylceramide concentration				Glucosylsphingosine concentration				MRI whole brain volume	Total modified SARA score	TMT difference Trail B versus Trail A (s)
		Plasma (μg/ml)		CSF (ng/ml)		Plasma (ng/ml)		CSF (pg/ml)				
		Change	Percentage change	Change	Percentage change	Change	Percentage change	Change	Percentage change	Percentage change		
Patient 1	1.1	−2.24	−45.8	−3.32	−47.4	−6.28	−71.5	−9.8	−46	**−0.23**	−3	**+3**
Patient 2	5.43	−5.31	−84	−3.53	−77.9	−8.67	−59.8	−14.3	−71.1	—	−1.5	−14
Patient 3	2.66	−4.19	−80.3	−3.32	−76.9	−8.07	−47.8	−17.3	−87.4	0.025	−0.5	**+24**
Patient 4	7.98	−3.68	−77	−7.02	−87.5	−4.5	−23.3	−32.7	−75.7	0.48	−2	−41
Patient 5	13.6	−6.69	−85.1	−13.3	−93	−31.3	−64	−35.7	−70.3	0.21	0	**+16**
Patient 6	6.32	−4.31	−82.5	−4.04	−80.2	−3.2	−56.1	−72	−72	**−0.52**	−1	−67
Patient 7	4.85	−5.49	−78.4	−4.95	−83.2	−18.9	−50.7	−23.2	−48	0.38	−3.5	−52
Patient 8	7.59	−4.7	−71.6	−8.95	−80.6	−33	−41.4	−30.2	−44.7	0.11	**+1.5**[a]	−50
Patient 9	<LLOQ	**+1.14**	**+13.7**	**+1.64**	**+37.1**	**+69**	**+43.4**	**+75.8**	**+313.2**	**−1.57**	−0.5	−2
Patient 10	7.62	−3.26	−78.2	−4.17	−80.7	−3.79	−60.3	−15.75	−69.7	**−0.22**	−1	−244
Patient 11	4.23	−3.97	−85.9	−4.7	−82.5	−22.5	−57.8	−53.5	−95.5	—	−1	**+14**

Values in bold denote worsening; the value in italics denotes no change. All other cells show improvement. (—) = no data available. In the total modified SARA score, each item of the SARA scale is scored on a 0 to 4 scale (lower score indicates improvement). Lower TMT score indicates improvement. Glucosylceramide healthy range: plasma <2.0–6.6 μg/ml, CSF 4.5–5.9 ng/ml. glucosylsphingosine healthy range: plasma <5 ng/ml, CSF undetectable.

[a]Calculation used the stance result for Week 26 instead of Week 52 due to knee pain and left great toe injury at Week 52.

patients were: headache (ten events in six patients), back pain (nine events in five patients), upper respiratory tract infection (two events in two patients), diarrhoea (two events in two patients), vomiting (two events in two patients) and acne (two events in two patients). Most adverse events were mild or moderate, transient and not considered related to venglustat or imiglucerase.

Discussion

After once-daily oral venglustat administration in adult GD3 patients, the agent crossed the blood–brain barrier as evidenced by venglustat in CSF detectable at 4 h post dose consistently over 1 year of treatment (excluding Patient 9). Furthermore, the addition of venglustat to existing imiglucerase regimens reduced CSF biomarkers of GD activity, including a marked decrease of the main disease biomarker (glucosylceramide) into the healthy reference range, after 4 weeks of treatment in all 11 patients, changes that were maintained throughout 1 year of treatment in the 10 patients in whom venglustat exposure was sustained. These reductions in glucosylceramide and glucosylsphingosine concentrations in the CSF demonstrate venglustat engagement with the drug target, UDP-glucose ceramide glucosyltransferase in the brain. These two glycosphingolipids are the immediate metabolic products of UDP-glucose ceramide glucosyltransferase, the biosynthetic reaction target on the *cis*-Golgi; glucosylceramide is the critical precursor of nearly all gluco-series glycosphingolipids. Venglustat also appeared to be safe and tolerable during 1 year of exposure in combination with imiglucerase, with most adverse events being mild or moderate, transient and not considered treatment-related; no patient discontinued treatment. The most frequently reported adverse events (headache and back pain) were probably related to the lumbar puncture procedure to obtain CSF for biomarker analysis.

As noted previously, Patient 9 had reduced venglustat plasma and CSF concentrations at Week 26 and beyond. The reason for reduced exposure could not be determined. The patient did not acknowledge difficulties with adherence when interviewed by the investigator, and no drug–drug interactions were identified.

During venglustat treatment, glucosylceramide concentrations decreased to below the normal range (Fig. 3A and B) and glucosylsphingosine concentrations decreased but did not normalize (Fig. 3C and D). No long-term safety concerns with low glucosylceramide levels have been observed in heterozygote mice.[40,41] or in long-term clinical trial follow-up of 393 patients (representing 1400 person-years) treated with the non-brain-penetrant glucosylceramide synthase inhibitor, eliglustat.[42] Furthermore, the principle of substrate reduction therapy depends on the fact that all patients with GD, irrespective of clinical phenotype (except the type 2 lethal neonatal form), have measurable residual *GBA1* activity.[43,44] Long-term follow-up of the LEAP patients for 208 weeks will provide additional insights on this issue. The fact that glucosylsphingosine did not normalize may be partly explained by the known lower efficiency of acid β-glucosidase in the hydrolysis of glucosylsphingosine compared with its cognate substrate, glucosylceramide.[45] Another explanation lies in the water-soluble nature of glucosylsphingosine, which partitions into the fluid phase after release by activated acid ceramidase in the lysosome.[46] While efflux of glucosylsphingosine into interstitial fluid and plasma precedes disposal in the urine and bile,[47] physical dissociation from residual lysosomal glucosylceramidase precludes acid hydrolysis. Further study is needed to understand the metabolic fate of glucosylsphingosine in patients with GD.

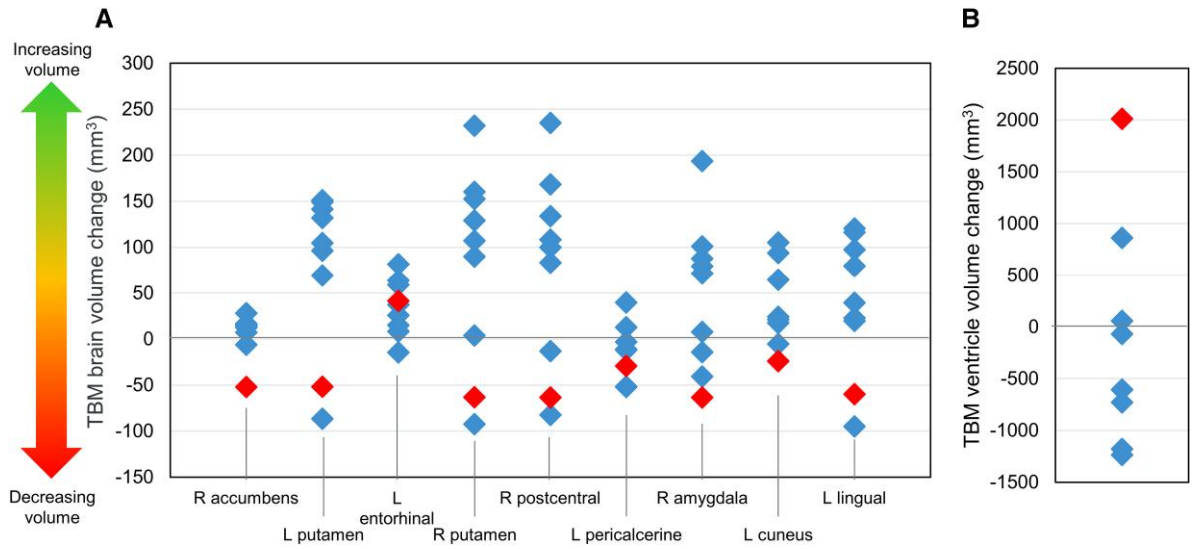

Figure 5 Tensor-based morphometry cycle at Week 52 visit. Top 10 regional brain volumes changes. (**A**) The nine brain regions with the greatest increases in volume for vMRI Group A (patients with adequate venglustat, shown as blue diamonds) compared with decreases in eight of these nine regions in Patient 9 (patient with low-to-undetectable venglustat exposure, shown as red diamonds). (**B**) The mean volume of the cerebral ventricles decreased in vMRI Group A, while in Patient 9, ventricular volume increased, reflecting a progressive loss of brain tissue. TBM = tensor-based morphometry.

Other investigational therapies for GD3

Several other approaches to treatment of neurological features of GD are currently in early development. Pharmacological chaperone therapy is an emerging strategy that uses chaperone molecules to assist in the folding of mutated enzymes and improve their stability and lysosomal trafficking.[48,49] Viral vector-based delivery of a functional *GBA1* gene to drive expression in a mouse model of neuronopathic GD has been shown to increase acid β-glucosidase activity, as well as increase the life span of treated animals, rescue the lethal neurodegeneration, normalize the locomotor behavioural defects and ameliorate the visceral pathology.[50] Small case series have shown that haematopoietic stem cell transplant can provide a permanent source of acid β-glucosidase to GD patients[51]; with successful engraftment, some patients with GD3 have been reported as showing no further neurological deterioration.[52] However, no clinical trials have assessed the safety and efficacy of this intervention in comparison with conservative measures (i.e. enzyme replacement therapy, substrate reduction therapy) now in use. While there are reports of benefit from transplantation of haematopoietic stem cells before neurological disease is apparent,[53] long-term follow-up in two intensely studied Swedish patients with the Norrbottnian variant and nine Swedish and UK neuronopathic GD patients revealed neurological deterioration after the procedure.[54,55] Investigation of the oral, small-molecule glucosylceramide synthase inhibitor, miglustat, for neuropathic GD was discontinued after it showed no clinical benefit for neurological manifestations of GD3.[17]

Regional brain volumes and connectivity

Before this study, there had been few reports of neuroimaging in GD3. Standard brain MRI in GD3 patients has been most often normal and remained so over time, except in patients with progressive myoclonic epilepsy who develop progressive brain atrophy.[12] More recently, rare reports of bilateral thalamic and dentate nuclei abnormalities have been described in children with GD3 but their relationship to the disease is unclear.[56] Diffusion tensor imaging in small groups of GD3 and GD1 patients showed decreased fractional anisotropy and increased mean diffusivity primarily in the middle cerebellar peduncles, but also in the superior cerebellar peduncles.[57] A larger study confirmed diffusion tensor imaging abnormalities in these areas and in the posterior thalamus and other white matter regions in 22 patients identified as GD1,[58] despite most having *GBA1* mutations typically associated with neuronopathic GD. Taken together, subtle white matter abnormalities that probably underlie functional connectivity disturbances are present in patients with GD3 even in the presence of normal standard brain MRI.

The current fMRI analysis indicated that patients with measurable venglustat exposure (fMRI Group A) developed greater coherence between posterior and anterior aspects of the brain, such that the entire brain became amenable to efficient information transfer. Increased functional connectivity in this group was most prominent within sensory, motor and cerebellar networks thought to be disrupted in GD1.[59] Specifically, disrupted connectivity has been observed in the right precentral gyrus in GD1 patients.[59] The LEAP data indicate that connectivity in this same brain region was restored following venglustat treatment and that the right precentral gyrus is a central node of enhanced connectivity at the regional and network levels. From a network perspective, precentral gyrus is the primary motor cortex and resides within sensorimotor RSN 6, which was also a primary site of enhanced connectivity after 1 year of venglustat treatment. Together, these results indicate the precentral gyrus represents an important node in the overall pattern of altered connectivity in GD.

Clinical improvements in ataxia and executive function could be a functional consequence of this enhanced sensorimotor coherence. Enhanced coherence may reflect evidence of a stronger treatment effect than is typically seen in clinical trials of neurodegenerative disorders, where stabilization or recovery of dysfunctional networks represent a positive outcome.[60,61] In patients with measurable venglustat exposure, progressive disruption in sensorimotor connectivity was not merely slowed but,

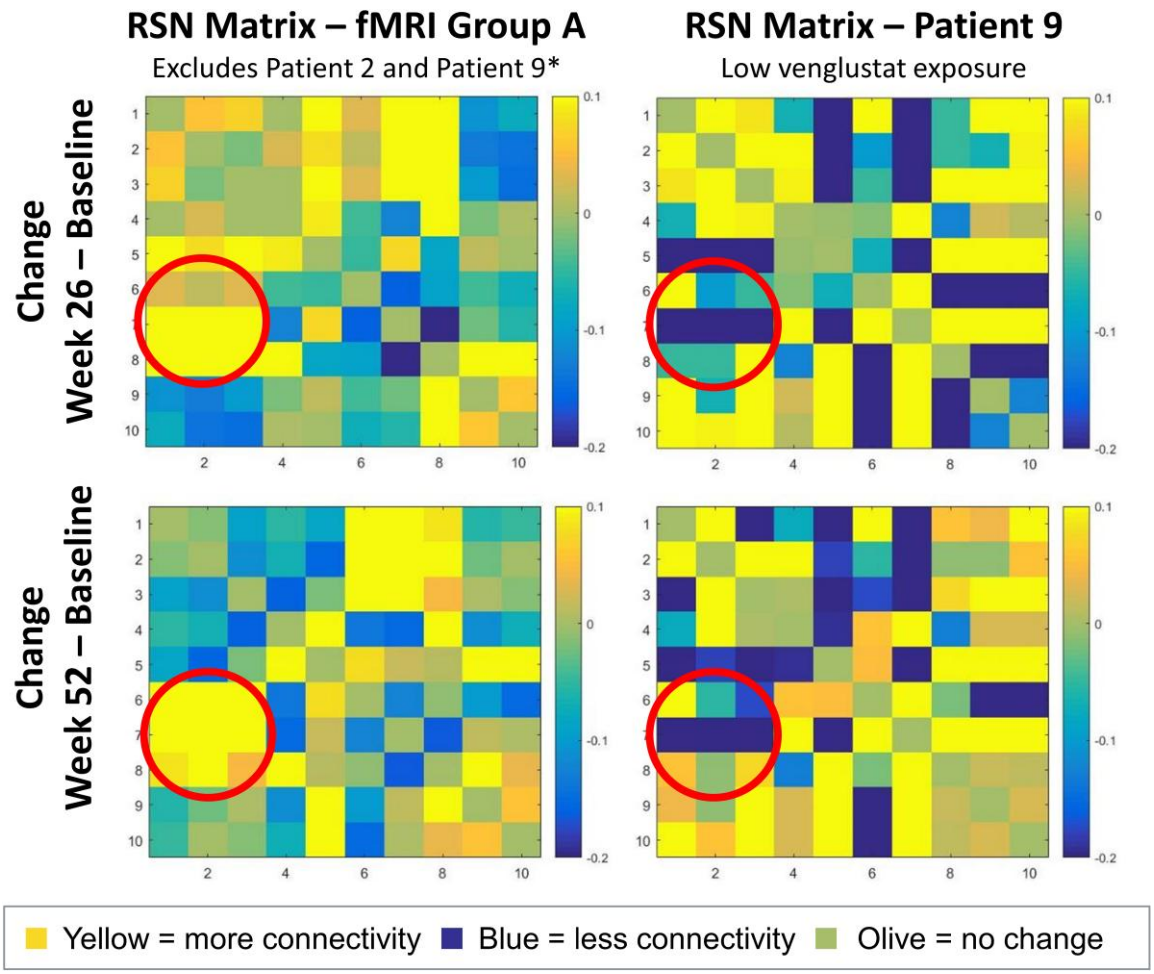

Figure 6 Change in connectivity between functional RSNs in fMRI group A versus Patient 9. Functional MRI Group A patients (i.e. adequate venglustat exposure) (*left*) demonstrated enhanced connectivity (yellow) within a cluster of spatially and behaviourally disparate nodes (RSNs 1,2,3 and 6,7,8). Patient 9 showed less connectivity (blue). Where apparent, sites of enhanced connectivity in Patient 9 (i.e. low-to-undetectable venglustat exposure) werecloser to the line of identity, reflecting increased correlation between neighbouring sets of brain regions (RSNs 6 and 8, 7 and 9). These results indicate that fMRI Group A demonstrated increasing coherence within a wider spatial distribution than the local changes observed in Patient 9. Note: RSN matrices report full correlation (*bottom half*) and partial correlation (*upper half*), with partial correlation reflecting the unique variance accounted for by two RSNs while controlling for the variance from the other eight RSNs. *Patient 9 did not have measurable venglustat exposure and Patient 2 did not have an fMRI performed.

notably, reversed. Improvements of this kind have been reported in studies of donepezil for Alzheimer's disease and ketamine for major depression, where changes in RSN connectivity with drug treatment correlated with neurological improvements.[62,63] In the patient with low venglustat exposure (Patient 9), enhanced connectivity was typically absent or reversed and, when present, appeared to be within a narrower set of anterior brain regions, although the pattern is inconsistent with an apparent decrease in ataxia (Fig. 4A).

It is noteworthy that the brain regions in which volume increased overlapped with the brain regions that showed increased connectivity, including the cerebellum, sensorimotor and cognitive regions. Prior studies have shown that changes in brain network connectivity can reflect macrostructural brain changes.[64] For example, juggling training improves visuo-motor coordination with increased grey matter volume in the occipito-parietal region.[65]

While change in brain volume in patients with GD3 has not been thoroughly studied, whole brain volume atrophy (i.e. loss of volume) has been reported in a few neuronopathic GD patients[66] and is frequently noted in other neurodegenerative diseases. Conversely, neurodegeneration is characteristically linked to an increase in ventricular volume. In a recent study of 1774 participants in the Mayo Clinic Study of Aging, increase in ventricular volume was associated with gait and cognition disturbance and was a predictive measure of current and future gait and cognitive performance.[67] In a vMRI study of patients with Alzheimer's disease, whole brain volume decreased at an annual rate of ~−1.4 to −1.6% and ventricular volume increased ~9.6 to 9.9%.[68,69] Of note, our patient who had low venglustat exposure (Patient 9) showed similar rates of change after 1 year: whole brain volume reduction of 1.57% and ventricular volume increase of 9.6%. This inverse relationship between ventricle volume and whole brain volume is consistent with brain parenchymal shrinkage in neurodegenerative diseases.[70] The absolute values of volume change should be interpreted with caution, since brain atrophy is also a function of age; they are also inconsistent with an apparent decrease in ataxia in Patient 9 (Fig. 4A). The patients with measurable and sustained venglustat exposure (vMRI Group A) had an increase in whole brain volume and a slight reduction in ventricle volume over 1 year of treatment. These findings were corroborated by measurements of

regional brain volumes, which show that for eight of the nine brain regions with the largest increases in volume, the corresponding regions in Patient 9 decreased in volume. Patients with measurable venglustat exposure displayed a slight increase in whole brain volume and a significant reduction in ventricle volume, which we contend is an indication that the treatment may have a positive effect on brain structure.

Neurological and neurocognitive manifestations

Total modified SARA score and difference between time to complete TMT Trail B minus time to complete Trail A improved during 1 year of treatment in most patients, suggesting potential for venglustat to ameliorate ataxia and neurocognitive deficits in GD3 patients, which needs to be validated and confirmed in future clinical studies. The low SARA scores at baseline reflect mild ataxia in this population. These patients exhibited mostly truncal ataxia with a wide-based gait and difficulty performing tandem gait or standing on one foot. The observed improvements in SARA scores were small and perhaps within the range of test-retest variability. Speech and appendicular movements were generally spared. TMT has been used extensively to evaluate executive function in a wide range of disorders including migraine,[71] brain injury, Alzheimer disease and other neuropsychiatric disorders.[72] Tasks requiring executive function activate distributed neural networks that prominently involve the prefrontal cortex, but also include the parietal cortex, basal ganglia, thalamus and cerebellum.[73] It is possible that the reduction in TMT and SARA scores in these patients is a clinical correlate of volumetric and fMRI improvement.

While receiving enzyme replacement therapy, cognition in adult GD3 patients was considered to remain stable or slowly decline.[12,15] In this study, however, a modest decline in function was detected on the Vineland II assessment. The apparent improvement in clinical features, regional brain volume and functional connectivity in patients with adequate venglustat exposure may be attributed to preserved neuronal plasticity in patients with GD3. The absence of improvement in adaptive behaviours as measured by Vineland II suggests that it is not sensitive enough to assess change over time in this population, a phenomenon similar to that observed using the Wechsler Intelligence Scales in patients with GD3.[14] On the other hand, we did not observe an improvement in saccadic eye movements, the neurological hallmark of neuronopathic GD. Our findings probably reflect absence or mild loss of cortical neurons in the cerebral hemispheres as reported in autopsied GD3 patients who did not suffer from progressive myoclonic epilepsy.[7,9] On the other hand, it is likely that loss of brain stem neurons in the nuclei responsible for eye movements was too extensive to permit recovery even after correction of the relevant glycosphingolipid metabolism. This may also indicate that the therapeutic regimen used in this study is incomplete or insufficient and can be further optimized.

Limitations

As the first study of venglustat in patients with GD3, this open-label, uncontrolled study had a small sample size, no untreated comparator group and comparative statistical testing was not carried out. While our results indicate a correlation between changes observed on fMRI and vMRI and neurological/clinical outcomes, the exact relationship and mechanisms remain to be elucidated. In addition, the natural history of neurological manifestations in patients with GD3 has not been fully elucidated. A full assessment of skeletal outcomes will require longer follow-up given that skeletal responses to treatment are known to evolve over several years[74] and the LEAP patients were already receiving long-term enzyme replacement therapy.

Conclusions

The addition of once-daily oral venglustat to imiglucerase for treatment of adults with GD3 showed an acceptable safety and tolerability profile, engagement with the proven molecular target in the brain and preliminary evidence of clinical stability with some informative, but intrinsically inconsistent, signals in selected biomarkers that require validation and confirmation in additional clinical studies. At present, however, we do not recommend off-label use of this compound outside clinical studies.

Acknowledgements

The authors thank the patients and their families who participated in this study, as well as the following Sanofi employees who contributed to this analysis: Vijay Modur, Samantha Walbillic, Nigel Crawford, Tanya Fischer, Allena Ji, Qi Zang, Lisa Underhill, Shirali Pandya and Selena Freisens. The authors thank Laurie LaRusso, MS, ELS (Chestnut Medical Communications) for medical writing funded by Sanofi.

Funding

The LEAP trial was funded and conducted by Sanofi.

Competing interests

R.S. is the lead principal investigator on the venglustat LEAP trial and receives research support and honoraria from Sanofi and Protalix Biotherapeutics. P.KM. is a principal investigator on the venglustat LEAP trial and the eliglustat ENGAGE trial, both sponsored by Sanofi. He reports membership on the International Collaborative Gaucher Group (ICCG) Gaucher Registry North American Advisory Board and receives research support, honoraria and travel reimbursement from Sanofi. T.M.C. is a principal investigator on the venglustat LEAP and AMETHIST trials and the former eliglustat ENCORE trial—all sponsored by Sanofi. He reports receiving honoraria, travel reimbursement and grant/research support from Shire (now Takeda) Pharmaceuticals. E.M. is a principal investigator on the venglustat LEAP trial and reports receiving fees and consultant honoraria from Actelion, Alexion, Orphazyme A/S, Sanofi and Takeda. H.I. reports grant/research support from Sanofi and Dainippon Sumitomo. D.S. is employed by Clario, the company paid by Sanofi to perform the functional and volumetric MRI analyses for the LEAP trial. J.B.H. is principal investigator on the venglustat LEAP trial and received honoraria/travel support from Amicus, Chiesi, Sanofi and Shire/Takeda. J.F.D., P.M., P.B.M., M.J.P., S.J.M.G. and J.S. report employment with Sanofi; some also own shares and/or stock options in the company.

Supplementary material

Supplementary material is available at *Brain* online.

References

1. Grabowski GA, Petsko GA, Kolodny EH, *et al*. Gaucher disease. In: Valle D Beaudet AL and Vogelstein B, eds. *OMMBID: The online*

metabolic and molecular bases of inherited disease. McGraw-Hill; 2013. Available at: https://ommbid.mhmedical.com/content.aspx?bookid=2709§ionid=225546056
2. Schiffmann R, Sevigny J, Rolfs A, *et al*. The definition of neuronopathic Gaucher disease. *J Inherit Metab Dis*. 2020;43:1056-1059.
3. Vellodi A, Tylki-Szymanska A, Davies EH, *et al*. Management of neuronopathic Gaucher disease: Revised recommendations. *J Inherit Metab Dis*. 2009;32:660-664.
4. Tylki-Szymanska A, Vellodi A, El-Beshlawy A, Cole JA, Kolodny E. Neuronopathic Gaucher disease: Demographic and clinical features of 131 patients enrolled in the International Collaborative Gaucher Group Neurological Outcomes Subregistry. *J Inherit Metab Dis*. 2010;33:339-346.
5. Grabowski GA, Zimran A, Ida H. Gaucher disease types 1 and 3: Phenotypic characterization of large populations from the ICGG Gaucher Registry. *Am J Hematol*. 2015;90(Suppl 1):S12-S18.
6. Nilsson O, Svennerholm L. Accumulation of glucosylceramide and glucosylsphingosine (psychosine) in cerebrum and cerebellum in infantile and juvenile Gaucher disease. *J Neurochem*. 1982;39:709-718.
7. Wong K, Sidransky E, Verma A, *et al*. Neuropathology provides clues to the pathophysiology of Gaucher disease. *Mol Genet Metab*. 2004;82:192-207.
8. Conradi NG, Sourander P, Nilsson O, Svennerholm L, Erikson A. Neuropathology of the Norrbottnian type of Gaucher disease. Morphological and biochemical studies. *Acta Neuropathol*. 1984;65:99-109.
9. Kaye EM, Ullman MD, Wilson ER, Barranger JA. Type 2 and type 3 Gaucher disease: A morphological and biochemical study. *Ann Neurol*. 1986;20:223-230.
10. Burrow TA, Sun Y, Prada CE, *et al*. CNS, lung, and lymph node involvement in Gaucher disease type 3 after 11 years of therapy: Clinical, histopathologic, and biochemical findings. *Mol Genet Metab*. 2015;114:233-241.
11. Weinreb NJ, Camelo JS Jr, Charrow J, *et al*. Gaucher disease type 1 patients from the ICGG Gaucher Registry sustain initial clinical improvements during twenty years of imiglucerase treatment. *Mol Genet Metab*. 2021;132:100-111.
12. Altarescu G, Hill S, Wiggs E, *et al*. The efficacy of enzyme replacement therapy in patients with chronic neuronopathic Gaucher's disease. *J Pediatr*. 2001;138:539-547.
13. Goker-Alpan O, Wiggs EA, Eblan MJ, *et al*. Cognitive outcome in treated patients with chronic neuronopathic Gaucher disease. *J Pediatr*. 2008;153:89-94.e4.
14. Steward AM, Wiggs E, Lindstrom T, *et al*. Variation in cognitive function over time in Gaucher disease type 3. *Neurology*. 2019;93:e2272-e2283.
15. Benko W, Ries M, Wiggs EA, Brady RO, Schiffmann R, Fitzgibbon EJ. The saccadic and neurological deficits in type 3 Gaucher disease. *PLoS ONE*. 2011;6:e22410.
16. Shayman JA. Eliglustat tartrate: Glucosylceramide synthase inhibitor treatment of type 1 Gaucher disease. *Drugs Future*. 2010;35:613-620.
17. Schiffmann R, Fitzgibbon EJ, Harris C, *et al*. Randomized, controlled trial of miglustat in Gaucher's disease type 3. *Ann Neurol*. 2008;64:514-522.
18. Cox TL, Lachmann R, Hollak C, *et al*. Novel oral treatment of Gaucher's disease with N-butyldeoxynojirimycin (OGT 918) to decrease substrate biosynthesis. *Lancet*. 2000;355(9214):1481-1485.
19. Marshall J, Sun Y, Bangari DS, *et al*. CNS-accessible Inhibitor of glucosylceramide synthase for substrate reduction therapy of neuronopathic Gaucher disease. *Mol Ther*. 2016;24:1019-1029.
20. Peterschmitt MJ, Crawford NPS, Gaemers SJM, Ji AJ, Sharma J, Pham TT. Pharmacokinetics, pharmacodynamics, safety, and tolerability of oral venglustat in healthy volunteers. *Clin Pharmacol Drug Dev*. 2021;10:86-98.
21. Schmitz-Hubsch T, du Montcel ST, Baliko L, *et al*. Scale for the assessment and rating of ataxia: Development of a new clinical scale. *Neurology*. 2006;66:1717-1720.
22. Tombaugh TN. Trail Making Test A and B: Normative data stratified by age and education. *Arch Clin Neuropsychol*. 2004;19:203-214.
23. MacPherson SE, Cox SR, Dickie DA, *et al*. Processing speed and the relationship between trail making test-B performance, cortical thinning and white matter microstructure in older adults. *Cortex*. 2017;95:92-103.
24. CUP. Community-University Partnership for the Study of Children, Youth, and Families. Review of the Vineland Adaptive Behavior Scales-Second Edition (Vineland-II). Edmonton, Alberta, Canada. 2011.
25. Hollak CE, van Weely S, van Oers MH, Aerts JM. Marked elevation of plasma chitotriosidase activity. A novel hallmark of Gaucher disease. *J Clin Invest*. 1994;93:1288-1292.
26. Ghauharali-van der Vlugt K, Langeveld M, Poppema A, *et al*. Prominent increase in plasma ganglioside GM3 is associated with clinical manifestations of type I Gaucher disease. *Clin Chim Acta*. 2008;389(1-2):109-113.
27. Zigdon H, Savidor A, Levin Y, Meshcheriakova A, Schiffmann R, Futerman AH. Identification of a biomarker in cerebrospinal fluid for neuronopathic forms of Gaucher disease. *PLoS ONE*. 2015;10:e0120194.
28. Pastores GM, Weinreb NJ, Aerts H, *et al*. Therapeutic goals in the treatment of Gaucher disease. *Semin Hematol*. 2004;41(4 suppl 5):4-14.
29. Biegstraaten M, Cox TM, Belmatoug N, *et al*. Management goals for type 1 Gaucher disease: An expert consensus document from the European working group on Gaucher disease. *Blood Cells Mol Dis*. 2018;68:203-208.
30. Maas M, van Kuijk C, Stoker J, *et al*. Quantification of bone involvement in Gaucher disease: MR imaging bone marrow burden score as an alternative to Dixon quantitative chemical shift MR imaging—Initial experience. *Radiology*. 2003;229:554-561.
31. Graham BL, Steenbruggen I, Miller MR, *et al*. Standardization of spirometry 2019 update. An official American Thoracic Society and European Respiratory Society technical statement. *Am J Respir Crit Care Med*. 2019;200:e70-e88.
32. Calmon G, Roberts N. Automatic measurement of changes in brain volume on consecutive 3D MR images by segmentation propagation. *Magn Reson Imaging*. 2000;18:439-453.
33. Smith SM, Beckmann CF, Andersson J, *et al*. Resting-state fMRI in the human connectome project. *Neuroimage*. 2013;80:144-168.
34. Power JD, Mitra A, Laumann TO, Snyder AZ, Schlaggar BL, Petersen SE. Methods to detect, characterize, and remove motion artifact in resting state fMRI. *Neuroimage*. 2014;84:320-341.
35. Allen EA, Erhardt EB, Damaraju E, *et al*. A baseline for the multivariate comparison of resting-state networks. *Front Syst Neurosci*. 2011;5:2.
36. Erhardt EB, Rachakonda S, Bedrick EJ, Allen EA, Adali T, Calhoun VD. Comparison of multi-subject ICA methods for analysis of fMRI data. *Hum Brain Mapp*. 2011;32:2075-2095.
37. Smith SM, Fox PT, Miller KL, *et al*. Correspondence of the brain's functional architecture during activation and rest. *Proc Natl Acad Sci U S A*. 2009;106:13040-13045.
38. Biswal B, Yetkin FZ, Haughton VM, Hyde JS. Functional connectivity in the motor cortex of resting human brain using echo-planar MRI. *Magn Reson Med*. 1995;34:537-541.
39. Giovagnoli AR, Del Pesce M, Mascheroni S, Simoncelli M, Laiacona M, Capitani E. Trail making test: Normative values from 287 normal adult controls. *Ital J Neurol Sci*. 1996;17:305-309.

40. Saadat L, Dupree JL, Kilkus J, *et al*. Absence of oligodendroglial glucosylceramide synthesis does not result in CNS myelin abnormalities or alter the dysmyelinating phenotype of CGT-deficient mice. *Glia*. 2010;58:391-398.
41. Yamashita T, Wada R, Sasaki T, *et al*. A vital role for glycosphingolipid synthesis during development and differentiation. *Proc Natl Acad Sci U S A*. 1999;96:9142-9147.
42. Peterschmitt MJ, Freisens S, Underhill LH, Foster MC, Lewis G, Gaemers SJM. Long-term adverse event profile from four completed trials of oral eliglustat in adults with Gaucher disease type 1. *Orphanet J Rare Dis*. 2019;14:128.
43. Pentchev PG, Neumeyer B, Svennerholm L, Groth CG, Brady RO. Immunological and catalytic quantitation of splenic glucocerebrosidase from the three clinical forms of Gaucher disease. *Am J Hum Genet*. 1983;35:621-628.
44. Aerts JM, Donker-Koopman WE, Brul S, *et al*. Comparative study on glucocerebrosidase in spleens from patients with Gaucher disease. *Biochem J*. 1990;269:93-100.
45. Vaccaro AM, Muscillo M, Suzuki K. Characterization of human glucosylsphingosine glucosyl hydrolase and comparison with glucosylceramidase. *Eur J Biochem*. 1985;146:315-321.
46. Yamaguchi Y, Sasagasako N, Goto I, Kobayashi T. The synthetic pathway for glucosylsphingosine in cultured fibroblasts. *J Biochem*. 1994;116:704-710.
47. van Eijk M, Ferraz MJ, Boot RG, Aerts J. Lyso-glycosphingolipids: Presence and consequences. *Essays Biochem*. 2020;64:565-578.
48. Kim YM, Yum MS, Heo SH, *et al*. Pharmacologic properties of high-dose ambroxol in four patients with Gaucher disease and myoclonic epilepsy. *J Med Genet*. 2020;57:124-131.
49. Fog CK, Zago P, Malini E, *et al*. The heat shock protein amplifier arimoclomol improves refolding, maturation and lysosomal activity of glucocerebrosidase. *EBioMedicine*. 2018;38:142-153.
50. Massaro G, Hughes MP, Whaler SM, *et al*. Systemic AAV9 gene therapy using the synapsin I promoter rescues a mouse model of neuronopathic Gaucher disease but with limited cross-correction potential to astrocytes. *Hum Mol Genet*. 2020;29:1933-1949.
51. Ringden O, Remberger M, Svahn BM, *et al*. Allogeneic hematopoietic stem cell transplantation for inherited disorders: Experience in a single center. *Transplantation*. 2006;81:718-725.
52. Somaraju UR, Tadepalli K. Hematopoietic stem cell transplantation for Gaucher disease. *Cochrane Database Syst Rev*. 2017;10:CD006974.
53. Ito S, Barrett AJ. Gauchers disease—A reappraisal of hematopoietic stem cell transplantation. *Pediatr Hematol Oncol*. 2013;30:61-70.
54. Machaczka M. Allogeneic hematopoietic stem cell transplantation for treatment of Gaucher disease. *Pediatr Hematol Oncol*. 2013;30:459-461.
55. Donald A, Björkvall CK, Vellodi A, *et al*. Thirty-year clinical outcomes after haematopoietic stem cell transplantation in neuronopathic Gaucher disease. *Orphanet J Rare Dis*. 2022;17:1056.
56. Perucca G, Soares BP, Stagliano S, Davison J, Chakrapani A, D'Arco F. Thalamic and dentate nucleus abnormalities in the brain of children with Gaucher disease. *Neuroradiology*. 2018;60:1353-1356.
57. Davies EH, Seunarine KK, Banks T, Clark CA, Vellodi A. Brain white matter abnormalities in paediatric Gaucher Type I and Type III using diffusion tensor imaging. *J Inherit Metab Dis*. 2011;34:549-553.
58. Kang H, Zhang M, Ouyang M, *et al*. Brain white matter microstructural alterations in children of type I Gaucher disease characterized with diffusion tensor MR imaging. *Eur J Radiol*. 2018;102:22-29.
59. Zhang M, Wang S, Hu D, *et al*. Altered brain functional network in children with type 1 Gaucher disease: A longitudinal graph theory-based study. *Neuroradiology*. 2019;61:63-70.
60. Sole-Padulles C, Bartres-Faz D, Llado A, *et al*. Donepezil treatment stabilizes functional connectivity during resting state and brain activity during memory encoding in Alzheimer's disease. *J Clin Psychopharmacol*. 2013;33:199-205.
61. Goveas JS, Xie C, Ward BD, *et al*. Recovery of hippocampal network connectivity correlates with cognitive improvement in mild Alzheimer's disease patients treated with donepezil assessed by resting-state fMRI. *J Magn Reson Imaging*. 2011;34:764-773.
62. Griffanti L, Wilcock GK, Voets N, *et al*. Donepezil enhances frontal functional connectivity in Alzheimer's disease: A pilot study. *Dement Geriatr Cogn Dis Extra*. 2017;6:518-528.
63. Ionescu DF, Felicione JM, Gosai A, *et al*. Ketamine-associated brain changes: A review of the neuroimaging literature. *Harv Rev Psychiatry*. 2018;26:320-339.
64. Zatorre RJ, Fields RD, Johansen-Berg H. Plasticity in gray and white: Neuroimaging changes in brain structure during learning. *Nat Neurosci*. 2012;15:528-536.
65. Draganski B, Gaser C, Busch V, Schuierer G, Bogdahn U, May A. Neuroplasticity: Changes in grey matter induced by training. *Nature*. 2004;427:311-312.
66. Chang YC, Huang CC, Chen CY, Zimmerman RA. MRI In acute neuropathic Gaucher's disease. *Neuroradiology*. 2000;42:48-50.
67. Crook JE, Gunter JL, Ball CT, *et al*. Linear vs volume measures of ventricle size: Relation to present and future gait and cognition. *Neurology*. 2020;94:e549-e556.
68. Schwarz AJ, Sundell KL, Charil A, *et al*. Magnetic resonance imaging measures of brain atrophy from the EXPEDITION3 trial in mild Alzheimer's disease. *Alzheimers Dement*. 2019;5:328-337.
69. Siemers ER, Sundell KL, Carlson C, *et al*. Phase 3 solanezumab trials: Secondary outcomes in mild Alzheimer's disease patients. *Alzheimers Dement*. 2016;12:110-120.
70. Apostolova LG, Babakchanian S, Hwang KS, *et al*. Ventricular enlargement and its clinical correlates in the imaging cohort from the ADCS MCI donepezil/vitamin E study. *Alzheimer Dis Assoc Disord*. 2013;27:174-181.
71. Vuralli D, Ayata C, Bolay H. Cognitive dysfunction and migraine. *J Headache Pain*. 2018;19:109.
72. Sanchez-Cubillo I, Perianez JA, Adrover-Roig D, *et al*. Construct validity of the Trail Making Test: Role of task-switching, working memory, inhibition/interference control, and visuomotor abilities. *J Int Neuropsychol Soc*. 2009;15:438-450.
73. Rabinovici GD, Stephens ML, Possin KL. Executive dysfunction. *Continuum (Minneap Minn)*. 2015;21(3 Behavioral Neurology and Neuropsychiatry):646-659.
74. Hughes D, Mikosch P, Belmatoug N, *et al*. Gaucher disease in bone: From pathophysiology to practice. *J Bone Miner Res*. 2019;34:996-1013.